

Frequency and time-domain measurements on humid sand and soil

M. K. ANIS*, A. K. JONSCHER

Royal Holloway and Bedford New College, University of London Egham, Surrey TW20 0EX, UK

Dielectric measurements are reported in the frequency range 10^{-3} – 10^5 Hz and time range 10^{-3} – 10^3 s on samples of sand and soil of different purity, i.e. washed and unwashed, and in a range of relative humidities (RH) between 7% and 97%. All samples show, at low frequencies, a tendency to low-frequency dispersion, with varying degrees of complications from other processes and with a strong influence of purity and RH. At high frequencies there is a low-loss response independent of purity and RH arising from the bulk grains, while at intermediate frequencies evidence is seen for the first time of “dipole-like” response due to the individual grains acting as “giant dipoles”. Time-domain measurements show nearly time-independent charging and discharging currents with “battery-like” response, proving the dominance of electrochemical processes. A discussion is given of the observed behaviour in terms of the current understanding of dielectric processes in humid systems.

1. Introduction

The electrical properties of humid granular media such as sand, soil, etc., have been extensively studied in the past under steady-state conditions. Their dynamic behaviour as function of frequency or time is much less well understood and it shows a strong dependence on the relative humidity (RH). Early studies [1, 2] do not cover the low-frequency region, while Olhoeft and co-worker [3, 4] cover low frequencies but do not give time-domain response. Research work carried out on humid sand by Shahidi and Jonscher [5] has shown the presence of dispersion at low frequencies and this has later opened up the wider study of conduction on humid surfaces [6]. In the present experimental research work, a systematic study of sand and soil samples, with different granular sizes, was carried out in the frequency range 10^{-3} – 10^5 Hz and in the time range from 10^{-3} – 10^3 s, under different conditions of relative humidity (RH) (7%–97%).

The difficulty in the interpretation of geophysical electrical measurements is deciding which of the many possible physical and chemical processes actually determine the observed response. It has been reported [3] that these processes fall into two broad classes: charge transport (conduction) and charge accumulation (polarization). However, wide-ranging experience shows [6] that the time and frequency behaviour of these processes shows fractional power-law dependences which are not expected by accepted theories.

The dynamic response of transport processes may be studied dielectrically by the application of an alternating signal and the measurement of the amplitude and phase of the resulting current, thus determining the complex admittance and hence capacitance. The dielectric response of a solid medium reflects the con-

tribution of the various polarizing species present – permanent and induced dipoles, electrons and ions, each of which is characterized by the specific dependence of its complex dielectric permittivity on the temperature, T , and frequency, ω . The frequency dependence of the real and imaginary components of the effective complex susceptibility, $\tilde{X}(\omega)$ expressed as [6, 7]

$$\tilde{X}(\omega) = \tilde{C}'(\omega) - C_{\infty} \quad (1)$$

where

$$\tilde{C}'(\omega) = C'(\omega) - iC''(\omega) \quad (2)$$

is the measured complex capacitance and C_{∞} is the high-frequency limit of the capacitance where the losses are insignificant.

Experimental evidence shows [6–12] that the “universal” form of dielectric response is characterized by a fractional power-law dependence on frequency

$$\tilde{X}(\omega) = A(i\omega)^{n-1} \quad (3)$$

where A is a constant and the exponent falls in the range $0 < n < 1$. The Kramers–Kronig relations require that real and imaginary components of $\tilde{X}(\omega)$ are the same functions of frequency, differing only by a constant, so that

$$X''(\omega)/X'(\omega) = \cot(n\pi/2) \quad (4)$$

which is the general property of the so called “universal” dielectric relation.

The limiting case of dielectric relaxation for which the exponent n assumes values close to zero is referred to as low-frequency dispersion (LFD), which implies that the system is highly lossy and that both the loss $X''(\omega)$ and the real part $X'(\omega)$ increase rapidly towards low frequencies almost as ω^{-1} .

* Permanent address: Physics Department, Karachi University, Karachi 75270, Pakistan.

An immediate consequence of the power-law Equation 3 in the frequency domain (FD) is the time-domain (TD) response to a step-function voltage in the charging and discharging modes which is the Fourier transform of Equation 3 and follows a power law in time

$$i(t) \propto t^{-n} \quad (5)$$

In the case of small values of n arising in LFD, Equation 5 implies very slowly time-varying charging and discharging currents which may be described as “quasi-d.c.” [13]. The basic difference between LFD and true direct current (d.c.) transport is that d.c. does not involve any storage of charge in the system, while LFD does. The implication of this is that a d.c.-conducting system must give a truly time-independent step-charging current in response to step-voltage excitation but it cannot give any discharge current. A corresponding illustration of this may also be seen in the frequency domain, where d.c. response gives a constant $X'(\omega)$ towards low frequencies, while LFD shows a massive rise, sometimes by several orders of magnitude. The frequency and time-domain behaviour of LFD system is shown schematically in Fig. 1 which includes the highly lossy LFD response as well as the more normal low-loss high-frequency universal behaviour for which the exponent n lies closer to unity.

2. Experimental procedure

Frequency and time-domain measurements were carried out on sand and soil samples in the range 10^{-3} – 10^5 Hz and 10^{-3} – 10^3 s, respectively, under different humid conditions from 7%–97% RH.

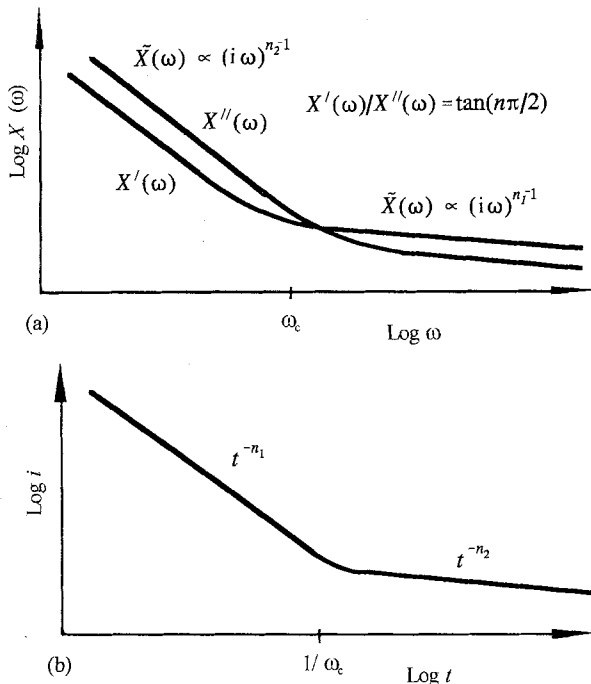


Figure 1 A schematic representation of the FD dielectric response, (a) showing LFD at low frequencies and a low-loss process at high frequencies. Both follow the same “universal” fractional power-law Equation 2, with the exponent n_2 close to zero at low frequencies and n_1 closer to unity at high frequencies. Note the parallelism of the $X'(\omega)$ and $X''(\omega)$ plots in logarithmic coordinates, following Equation 4. (b) The corresponding TD response with the characteristic nearly time-independent current at longer times.

The materials used were (i) agricultural soil from Harapa (Pakistan), (ii) sand used as building material from Karachi (Pakistan). These materials were sieved to obtain different granular sizes and were used either washed (W) or unwashed (U). The Harapa soil was sieved to $d \leq 45 \mu\text{m}$, and $45 \mu\text{m} < d < 0.5 \text{ mm}$. Malir sand was sieved to $0.5 < d < 1 \text{ mm}$.

Thorough washing of these materials, by shaking in a glass bottle, was carried out in hot and cold tap water and then in distilled water. Samples were shaken for 15–20 min up to seven times a day for sand and once a day for soil which took much longer time to segregate from water. These samples were then left in tap/distilled water overnight, and the washing process was repeated, up to 5 days for sand and 2 weeks for soil, until the water remained clear after shaking.

Especially designed PTFE tubular sample holders with internal diameter 12 mm were used for the measurements. For electrical contacts, two stainless steel hollow cylinders with outer diameter 12 mm were used to plug in at both ends of the sample holder. One end of each cylinder was welded with stainless steel wire gauze to facilitate more intimate contacts with the material and to provide easy access for circulation of humid air. For external connections, PTFE-coated silver-plated copper wire type 0.2 mm was soldered at the other end of the cylinder, which was then connected to 50 Ω coaxial cable using BNC connectors. The distance between the two electrodes was kept the same, 10 mm, in all the sample holders.

A total of eight sample holders was prepared, for Malir sand (M) and Harapa soil (H), to hold specimens arranged as shown in Table I. All these samples were then placed in a desiccator to maintain different humid conditions, using a saturated mixture of different salts, at room temperature.

Frequency domain measurements were carried out using a Solartron frequency response analyser (FRA) 1250 in conjunction with a Chelsea dielectric interface [14]. The results were plotted in the form of real and imaginary components of the complex capacitance $C'(\omega)$ and $C''(\omega)$ as functions of frequency in logarithmic coordinates. The numerical data were stored on disc for further processing if required, for example the subtraction of C_∞ and of the d.c. contribution, G_0 .

All measurements were made at room temperature with 1 V r.m.s. signal and zero d.c. bias. On the whole, we were able to ascertain good reproducibility of results after humidity cycling.

After completion of the FD measurements at 97% RH on the sand and soil samples, the same samples were used without changing any parameters for TD measurements, which were carried out in the range

TABLE I. Samples of sand and soil used in the present study

Unwashed			
2 sand	$\leq 1 \text{ mm K-UM12}$	and	$\leq 0.5 \text{ mm K-UM34}$
2 soil	$\leq 45 \mu\text{m K-UH56}$	and	$> 45 \mu\text{m K-UH78}$
Washed			
2 sand	$\leq 1 \text{ mm K-WM910}$	and	$\leq 0.5 \text{ mm K-WM1112}$
2 soil	$\leq 45 \mu\text{m K-WH1314}$	and	$> 45 \mu\text{m K-WH1516}$

10^{-3} – 10^3 s. The equipment used was a Chelsea time-domain instrument.

3. Results and discussion

3.1. Frequency domain

In the frequency-domain measurements the $C'(\omega)$ and $C''(\omega)$ plots for all U and W samples of sand and soil show LFD below a characteristic cross-over frequency, ω_c , at which $C''(\omega)$ crosses $C'(\omega)$. Because the high-frequency $C'(\omega)$ depends little on frequency and is almost independent of RH, ω_c is a measure of the “strength” of the LFD process. In the present experimental results the $\tilde{C}(\omega)$ behaviour may be seen as the superposition of three separate partially overlapping processes shown in Fig. 2a–c, whose relative dispersion in frequency varies according to RH and to the nature of the sample. Process I, Fig. 2a, dominates at high frequencies and is weakly dependent on frequency, RH and on washing. Process II, Fig. 2b, is

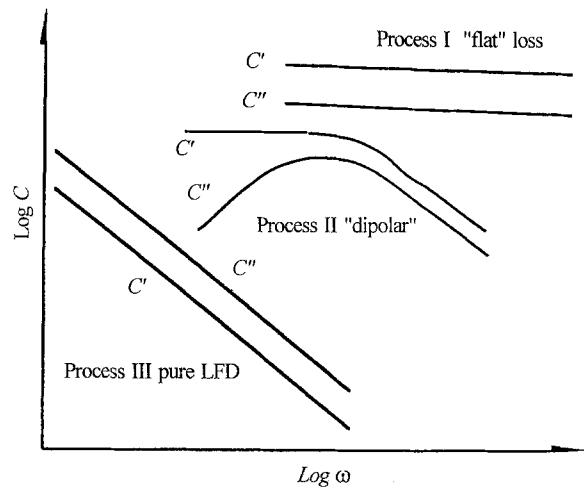


Figure 2 A schematic representation of the three principal types of dielectric relaxation found in sand and soil samples. Type I is a “flat” almost frequency-independent loss dominant at high frequencies, the dipolar Type II may be seen at intermediate frequencies and Type III is the LFD dominating at low frequencies.

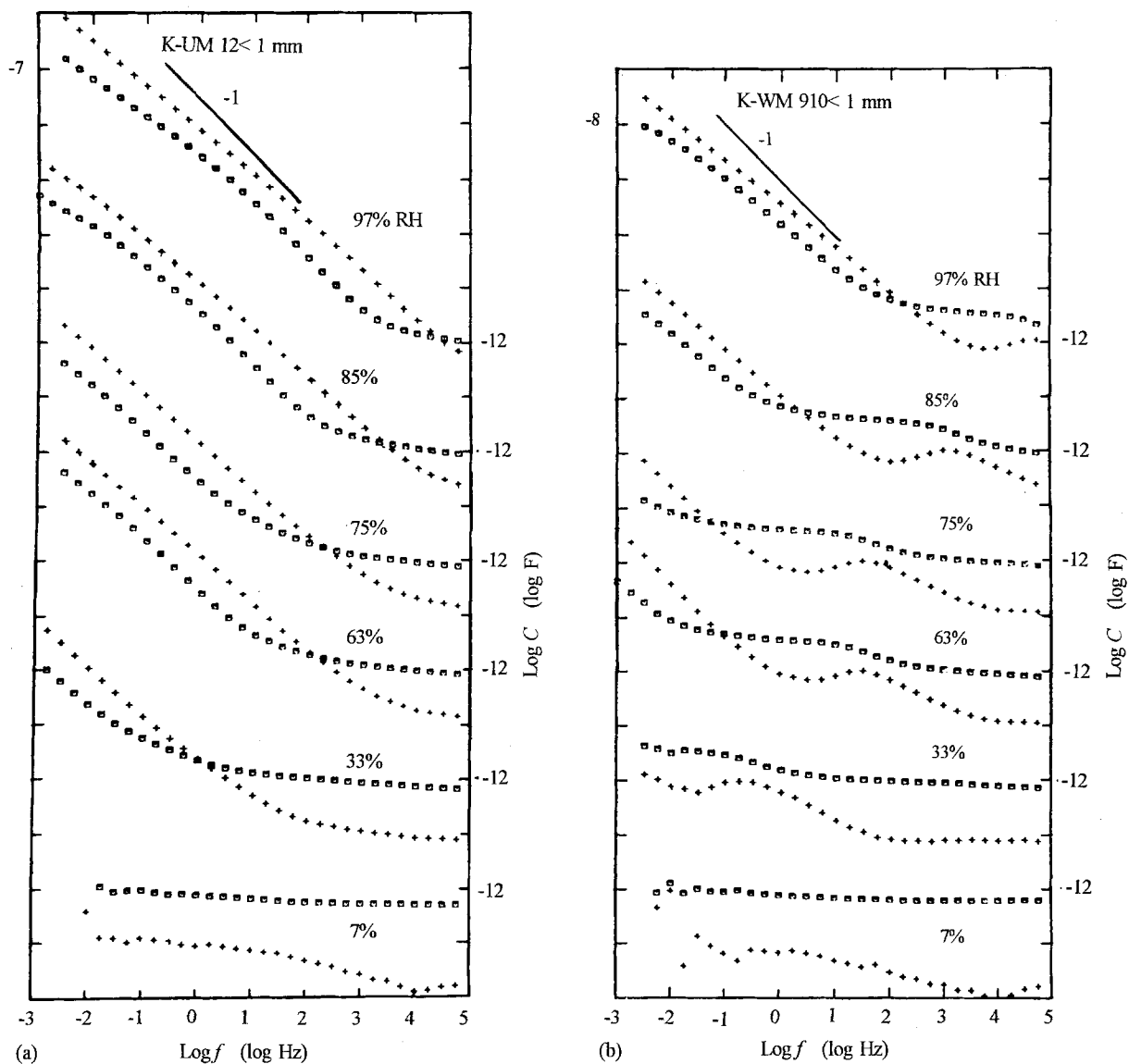


Figure 3 Log-log representation of the frequency dependence of the components (\square) $C'(\omega)$ and ($+$) $C''(\omega)$ of the complex capacitance of (a) unwashed and (b) washed Malir sand samples with grain size $0.5 < d < 1$ mm. The individual sets of data corresponding to different humidities are displaced vertically for clarity and typical capacitance values are indicated.

evidence of "dipolar" phenomena and shifts towards higher frequencies with increasing RH. Process III, Fig. 2c, dominating at low frequencies is strongly dispersive with a slope approaching -1 and is strongly RH dependent. This process may be "pure" LFD in which case the logarithmic $C'(\omega)$ and $C''(\omega)$ plots are parallel straight lines with a separation given by the ratio in Equation 4, or their shapes may be more complicated by the presence of series/parallel processes.

Figs 3-6 show the logarithmic plots of frequency dependence of $C'(\omega)$ and $C''(\omega)$ for U and W sand and soil samples under different humidity, the individual plots for different humidities being displaced vertically to avoid overcrowding.

Fig. 3a and b show U and W $d < 1$ mm Malir sand, respectively. The high-frequency limit of $C'(\omega)$ is approximately the same, is weakly dependent on RH and is of the order of 1 pF for both U and W sand, showing

that the effect of impurities is almost negligible. By contrast, the low-frequency values for U fall two decades higher than for W. The 7% RH data show a virtually "flat" frequency-independent loss, which is a characteristic feature of all low-loss materials. Fig. 3a shows the onset of the strongly dispersive Process III which rapidly increase in magnitude with rising RH. In the W samples of Fig. 3b, the lower level of the dispersive Region III reveals the presence of the dipolar Process II.

Fig. 4a and b present data for U and W Malir sand of $d < 0.5$ mm, with all three processes visible. Again Process II is more clearly seen in the U sample. Although the HF limit of $C'(\omega)$ is similar for U and W samples, at low frequencies U is two decades higher than W. In both U and W the HF process is impurity insensitive. In U $C'(\omega)$ and $C''(\omega)$ the LFD response follows effectively the pure power law with $K-K$ compatible ratio, and a slight deviation appears at highest

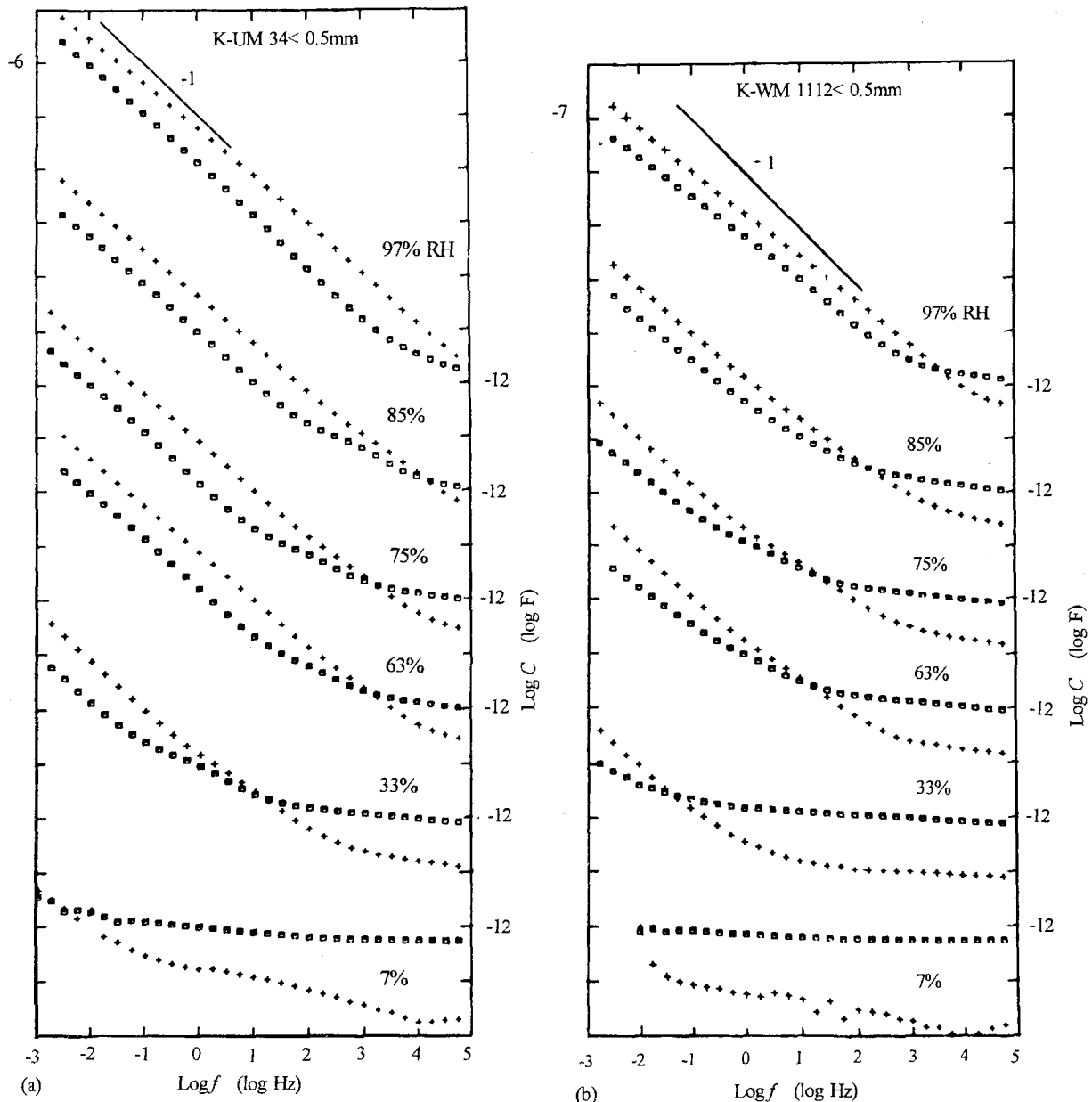


Figure 4 Log-log representation of the frequency dependence of the components (\square) $C'(\omega)$ and ($+$) $C''(\omega)$ of the complex capacitance of (a) unwashed and (b) washed Malir sand samples with grain size $d < 0.5$ mm. The individual sets of data corresponding to different humidities are displaced vertically for clarity and typical capacitance values are indicated.

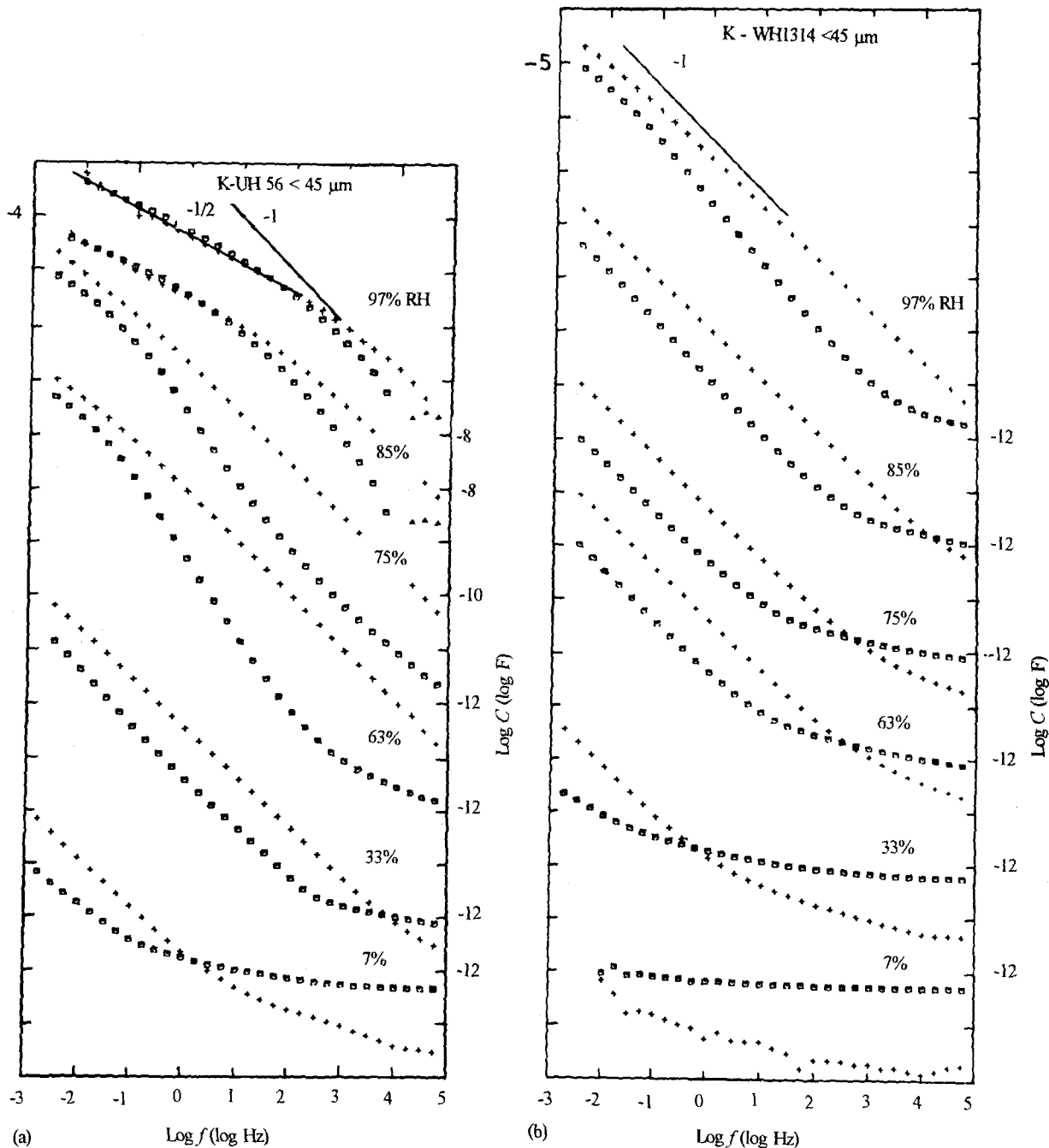


Figure 5 Log-log representation of the frequency dependence of the components (\square) $C'(\omega)$ and ($+$) $C''(\omega)$ of the complex capacitance of (a) unwashed and (b) washed Harapa soil with grain size $d \leq 45 \mu\text{m}$. The individual sets of data corresponding to different humidities are displaced vertically for clarity and typical capacitance values are indicated.

RH. The behaviour of the W samples, which are much less dispersive, is rather more complicated.

Fig. 5a and b show the data for U and W $d \leq 45 \mu\text{m}$ Harapa soil samples. The HF values of $C'(\omega)$ are now more strongly RH dependent than in sand and this is clearly due to a more rapid rise of Process III which swamps Processes I and II. The effect of RH is even more pronounced at lower frequencies where a $-1/2$ slope sets in at the highest humidities. Soil evidently contains more ionic impurities than does sand, and this may be due to the presence of humic acid in soil. Although the soil was washed thoroughly, the presence of organic materials makes it difficult to remove ionic impurities.

Fig. 6a and b give data for U and W $d > 45 \mu\text{m}$ Harapa soil. Although the overall behaviour of U is

close to that shown in Fig. 5a, the $C'(\omega)$ and $C''(\omega)$ values are comparatively higher in Fig. 6a at and above 85% RH. Again a $-1/2$ low-frequency slope at the highest humidity represents a definite trend, and Process II is swamped by LFD at high RH.

3.2. Time domain

In common with all other observations on charging and discharging currents [6] the magnitude of $i_c(t)$ depends on the charging voltage V_a , while $i_d(t)$ are only slightly voltage dependent. Fig. 7 shows a representative sample of the data for $i_c(t)$ and $i_d(t)$ for a range of charging voltages, for unwashed sand and washed soil, where $i_c(t)$ are seen to be independent of time, while $i_d(t)$ show a gradual fall at longer times. In broad

This clearly represents a "battery-like" behaviour. The magnitudes of the discharge currents and of R_s vary strongly between different samples, and Table II gives a summary of the results. The most sensitive parameter there, is the resistance, R_s , and it is evident that there is a very large (two decades) difference between the R_s values for washed and unwashed sand, and a comparatively much smaller difference for washed

(6b)

$$i_a(t) = V_0/R_s$$

horizontal lines

where the $i_a(t)$ is independent of V_a and is approximately given by the ratio V_a/R_a which is shown as

(6a)

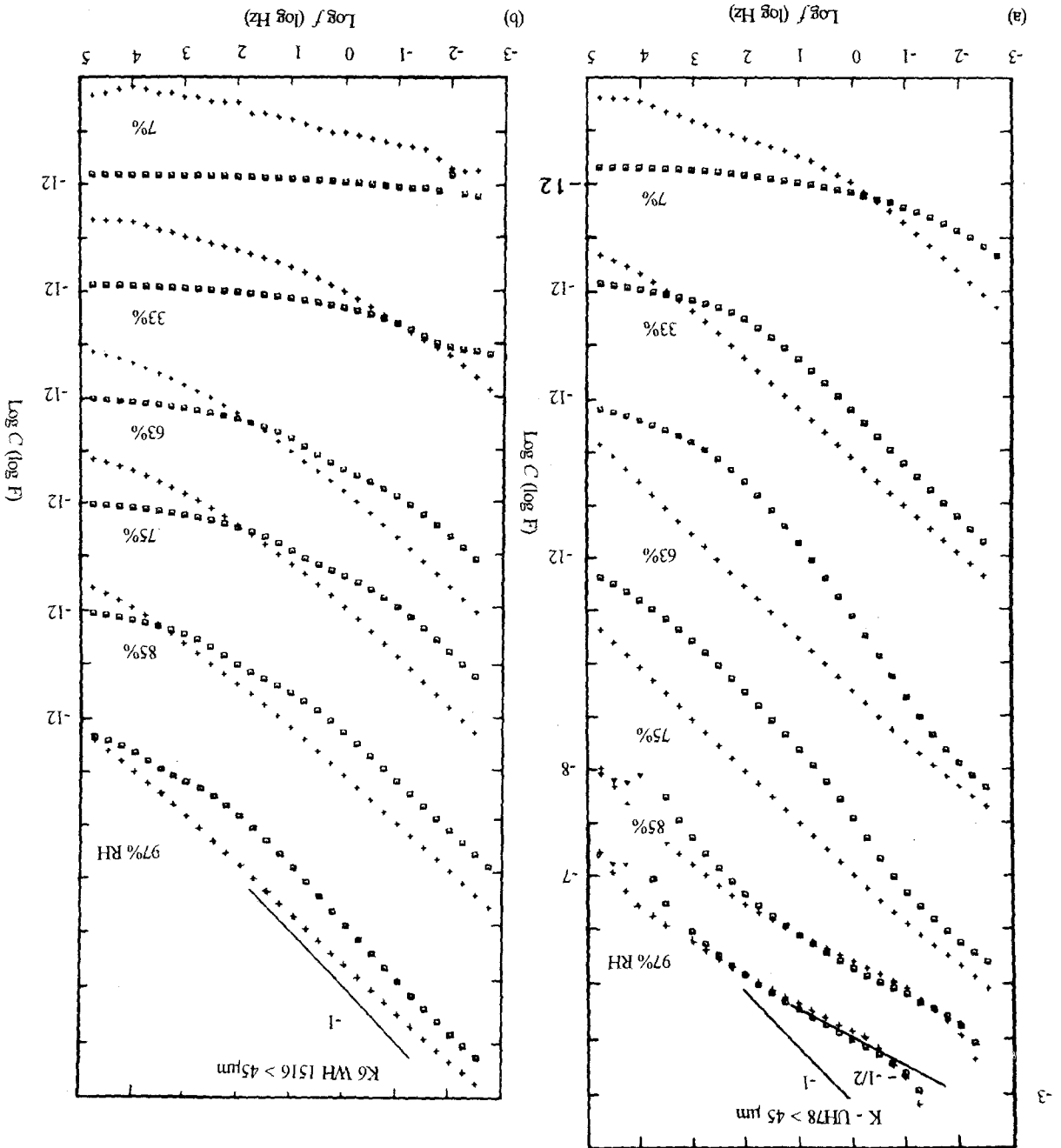
$$i_c(t) = (V_a - V_0)/R_s$$

voltage axis of between 1 and 3 V

in Fig. 7, where $i_c(t)$ is seen to rise linearly with V_a . Fig. 8 shows the relevant plots for the same samples as brings out the characteristic features of these currents. Plotting the values of $i_c(t)$ and $i_a(t)$ taken at some arbitrary time, say 1 s, against the charging voltage indicating the exhaustion of the stored charge.

terms, there is no large difference between the $i_c(t)$ and $i_a(t)$ behaviour of different soil and sand samples - in this respect the $C(\omega)$ are more informative. It is noteworthy, however, that for low charging voltages - some 3 V - there is a near-coincidence of $i_c(t)$ and $i_a(t)$ which later separate in magnitude. The charging currents are almost independent of time, with small variations both up and down, while the discharging currents are falling rapidly after approximately 10 s, indicating the exhaustion of the stored charge.

Figure 6 Log-log representation of the frequency dependence of the components (□) $C''(\omega)$ and (+) $C''(\omega)$ of the complex capacitance of (a) unwashed and (b) washed Harapa soil with grain size $45 \mu\text{m} < d < 0.5 \text{mm}$. The individual sets of data corresponding to different humidities are displaced vertically for clarity and typical capacitance values are indicated.



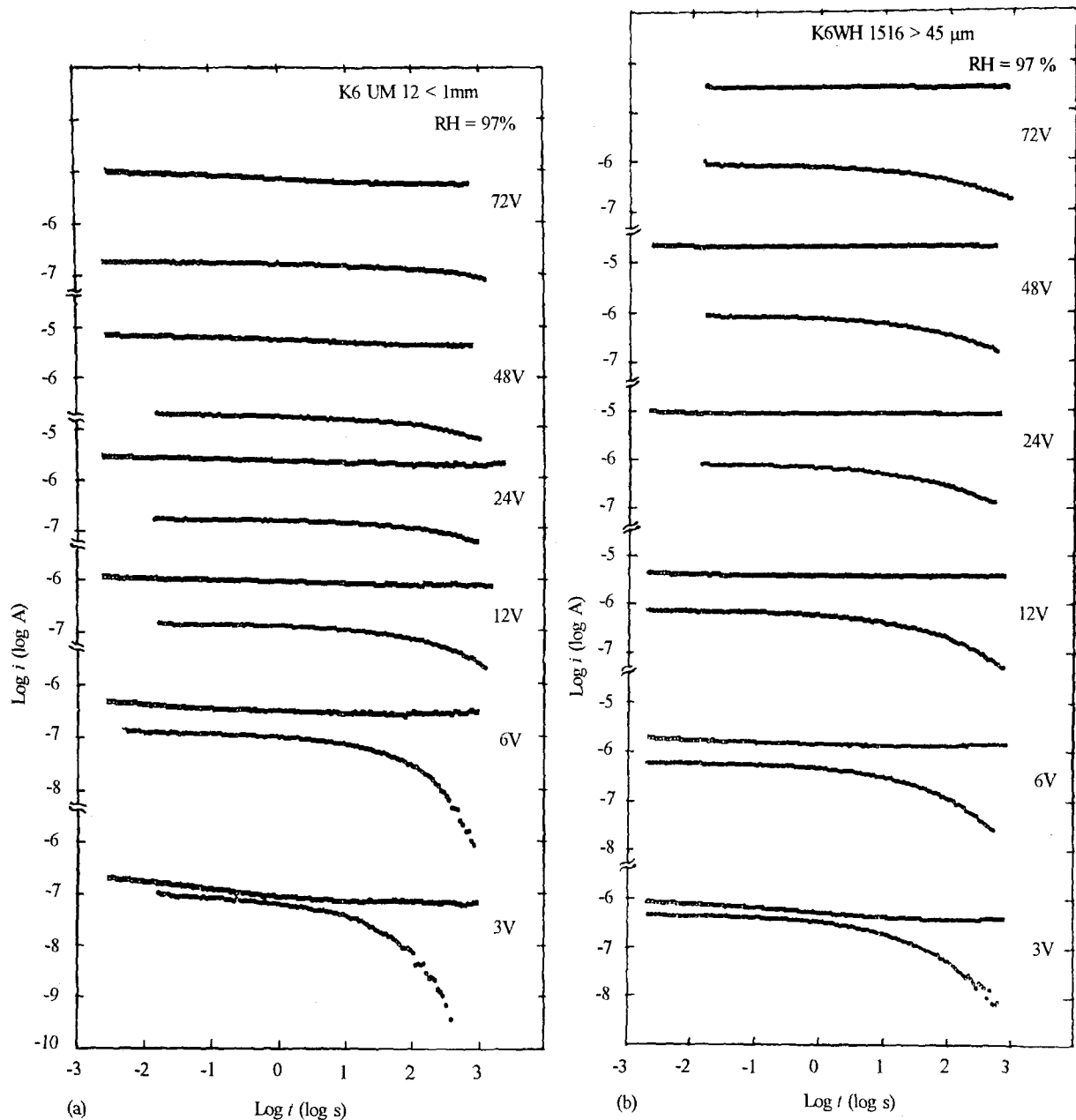


Figure 7 The time dependence of the (\square) charging currents $i_c(t)$ and (\circ) discharging currents $i_d(t)$ for a sample of (a) unwashed sand and (b) washed soil.

TABLE II

Sample	R_s (M Ω)	V_0 (V)	V_0/R_s (nA)	i_d (nA)
Sand < 1 mm unwashed	10	2	200	160
Sand < 1 mm washed	180	3	17	12
Sand < 0.5 mm unwashed	2.3	2	800	600
Sand < 0.5 mm washed	160	3	20	26
Soil > 45 μ m unwashed	0.8	0.5	600	400
Soil > 45 μ m washed	1.5	1	700	1200
Soil < 45 μ m unwashed	0.8	0.5	600	260
Soil < 45 μ m washed	2.5	3	1200	700

and unwashed soil, suggesting that the washing procedure is much more effective in removing impurities from sand than from soil. This is especially evident from the logarithmic chart in Fig. 9. Apart from that, there is no significant difference between the larger and smaller grain sizes of both sand and soil.

It is not possible to attach much significance to the values of V_0 , because these are subject to a considerable uncertainty regarding the exact magnitude of the intercept. For the same reason, the ratio V_0/R_s should not be regarded as very reliable to within a factor of 2 or so.

4. Conclusions

The behaviour of our samples of sand and soil shows most of the characteristic features of humid media, as described earlier. The $i_c(t)$ curves are virtually time-independent and, while $i_d(t)$ are likewise almost constant up to some tens of seconds, they then fall rapidly indicating the exhaustion of the stored charge. These results clearly show the effect of chemical battery-like processes, characterizing LFD behaviour in general [6] and the excellent agreement with the battery Equations 6a and b lends further support to this viewpoint.

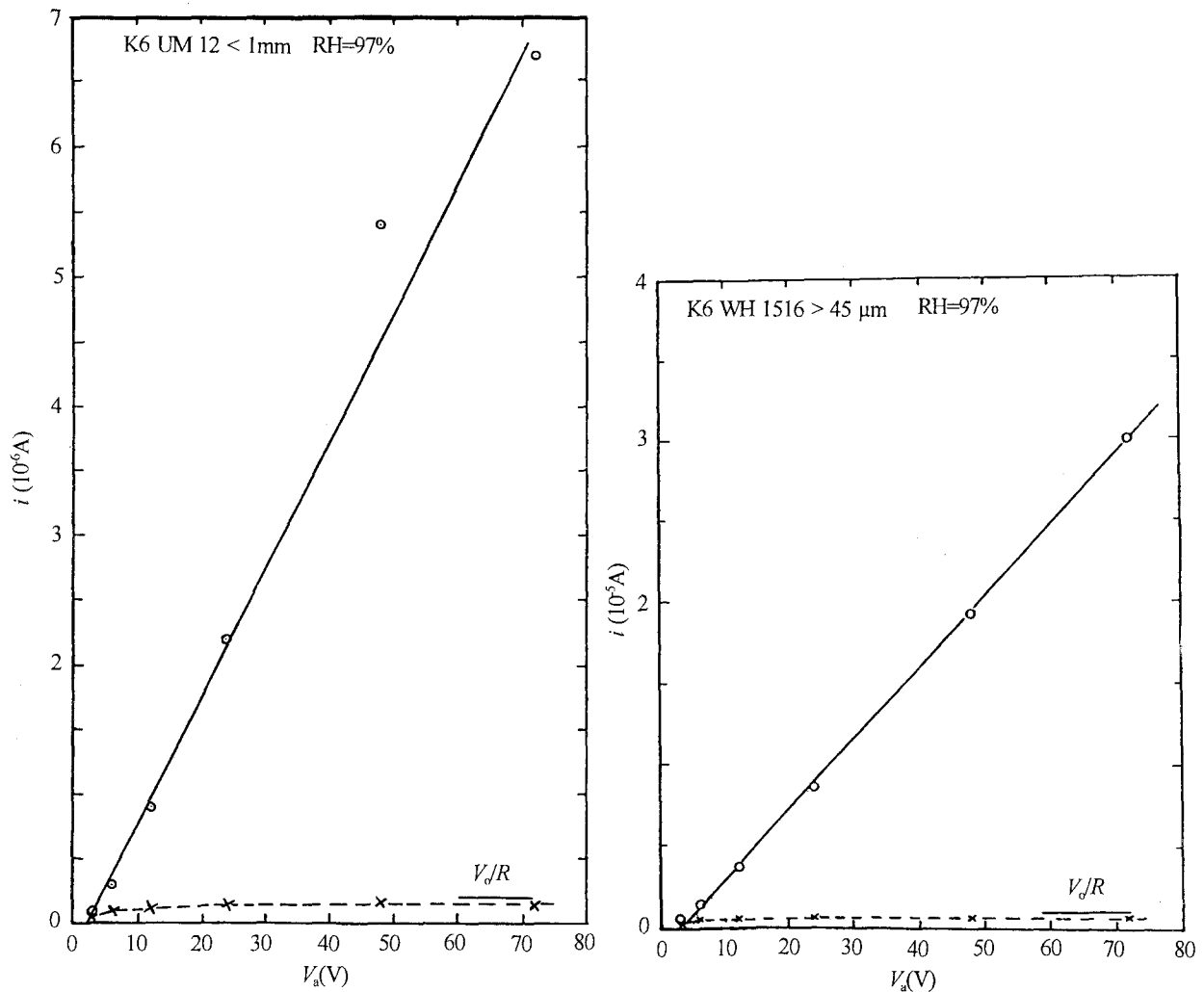


Figure 8 The dependence on the charging voltage, V_d , of the (○) charging and (×) discharging currents for the same samples of (a) unwashed sand and (b) washed soil as in Fig. 7.

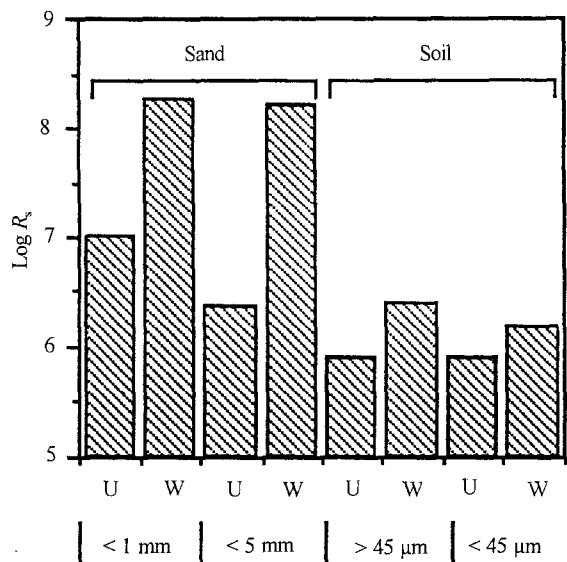


Figure 9 A diagrammatic representation of the logarithm of the series resistance, R_s , of washed (W) and unwashed (U) sand and soil samples are presented in Table II.

The significant new result derived from the present work is the effect of external contamination as manifested by the relative behaviour of washed and

unwashed samples. The high-frequency values of $C'(\omega)$ and $C''(\omega)$ are virtually independent of contamination, while the lower-frequency behaviour is strongly influenced by it. This suggests that the high-frequency behaviour is little affected by the surface transport and this is confirmed by the independence of these data of RH. The conclusion here must be that the high-frequency behaviour is typical of the mass of sand or soil, with some influence of the finite packing density, but with no other effects due to contacts, etc.

While some of the data for sand and soil, especially the lower-conducting washed ones, show "pure" LFD behaviour with parallelism of $C'(\omega)$ and $C''(\omega)$ data, other data depart from this pattern, showing deviations due to complicating features arising from the presence of series/parallel processes.

The soil samples show markedly higher conductance and capacitance than the sand samples by up to four decades in both washed and unwashed samples, suggesting that the soil contains many more ionic species which are bound in the organic matter and are very difficult to wash out. The most strongly conducting unwashed soil samples show a qualitative change of low-frequency behaviour towards exponents $n = 1/2$, which might be associated with diffusive pro-

cesses, although this is not necessarily the only explanation.

It is very likely that the lowering of the slope of the $C'(\omega)$ and $C''(\omega)$ at the lower frequencies in the highly conducting unwashed samples is due to the contacts being unable to cope with the rapid transfer of charge on the highly conducting grains.

A completely novel result regarding the behaviour of granular media is the evidence for the "dipolar" Process II which is visible wherever the Process III is not dominant over it. The most evident interpretation of this behaviour is the effect of individual grains acting as "giant dipoles" due to charge transport on the surface with very imperfect contacts between individual grains. This effect is most clearly visible in washed sand samples in which the LFD process is relatively suppressed.

The precise nature of the chemical reactions determining the behaviour of humid granular media is not known at the present time and neither are the relative roles of grain and contact transport. Our samples may be regarded as large assemblies involving parallel/series combinations of grains making very weak contacts with one another. The classical picture of a contact between two solids involves the concept of a contact area which is given by the force between the members divided by the yield stress. It is doubtful, however, if this picture is valid in the case of our humid sand and especially of soil with its additives of organic matter. It is probable that humidity may create an effective area of contact which exceeds the "true contact" area, possibly by a large factor and it is this process that dominates the "spreading resistance" of the grains.

Acknowledgement

One of the authors (MKA) is grateful to the Overseas Development Administration/The British Council, for financial support during a six-monthly stay at this College and for financing of some of the equipment used in the present work.

References

1. J. KEYMEULEN and W. DEKEYER, *J. Chem. Phys.* **27** (1957).
2. B. F. HOWELL and P. H. LICASTER, *Amer. Mineral.* **46** (1961).
3. G. R. OLHOEFT and J. H. SCOTT, "Nonlinear Complex Resistivity Logging" SPWLA-21st Annual Logging Symposium, 8-11 July 1980.
4. G. R. OLHOEFT, *Geophysics* **50** (1985) 2492.
5. M. SHAHIDI, J. B. HASTED and A. K. JONSCHER, *Nature* **258** (1975) 595.
6. A. K. JONSCHER, *J. Mater. Sci.* **26** (1991) 1618.
7. A. K. JONSCHER, "Dielectric Relaxation in solids" (Chelsea Dielectric Press, London, 1983).
8. A. R. HAIDAR and A. K. JONSCHER, *J. Chem. Soc. Faraday Trans. 1* **82** (1986) 3535.
9. A. K. JONSCHER and A. R. HAIDAR, *ibid.* **82** (1986) 3553.
10. A. K. JONSCHER and BIRJEES NAFIS AYUB, *J. Mater. Sci.*, in press.
11. E. F. OWEDE and A. K. JONSCHER, *J. Electrochem. Soc.* **135** (1988) 1757.
12. N. BANO and A. K. JONSCHER, *J. Mater. Sci.* **27** (1992) 1672.
13. L. A. DISSADO and R. M. HILL, *J. Chem. Soc. Faraday Trans. 2* **80** (1984) 291.
14. J. PUGH, Dielectric Materials, Measurements and Applications, IEE Publ. 239 (1984) p. 247.

Received 12 October

and accepted 19 November 1992